SORPTION OF OXYGEN ON Cu(111)–Ni SURFACES AND ITS REACTION WITH HYDROGEN

C.M.A.M. MESTERS *, A. DE KOSTER, O.L.J. GIJZEMAN and J.W. GEUS

Van 't Hoff Laboratory, University of Utrecht, Padualaan 8, 3584 CH Utrecht, The Netherlands

The interaction of O_2 with a Cu(111)–Ni alloy and the reaction of sorbed oxygen with H_2 has been investigated with ellipsometry and AES. The surface alloys were prepared by dissociation of nickel carbonyl on a clean Cu(111) surface. Sorption of O_2 can be described by a precursor state model for dissociative chemisorption followed by a first order reaction of adsorbed oxygen atoms to incorporated oxygen atoms. The initial sticking probability is 10^{-3} at room temperature and increases with increasing crystal temperature. The first chemisorption of O_2 on a freshly prepared alloy surface causes an irreversible surface reconstruction. The amount of oxygen in the near surface layer decreases with increasing crystal temperature. The reaction of sorbed oxygen with H_2 can be described by a nucleation and growth mechanism with a time dependent number of growth centers. The rate is strongly affected by an operating ionisation gauge.

1. Introduction

Cu–Ni alloys have been the subject of many investigations, especially in relation to surface segregation. Although Cu–Ni catalysts have been studied in a large number of reactions, the study of the reactivity of single crystals is mainly limited to the adsorption of CO and H_2. Very few authors [1–3] have dealt with the adsorption of O_2, although this process has been shown to be different on pure Cu and Ni [4,5]. To our knowledge no data are available in the literature about the reactivity of adsorbed oxygen on Cu(111)–Ni single crystal surfaces towards CO and H_2. Since the reactivity of sorbed oxygen on the pure metal surfaces is well known for Cu [4,6–8] and Ni [5,9,10] it would be interesting to obtain similar information about the reactivity of the alloy surface.

As we have shown before [11], Cu(111)–Ni surface alloys prepared by dissociation of nickel carbonyl are enriched in Cu, in the same way as

---

* Present address: Koninklijke/Shell Laboratorium (Amsterdam), Badhuisweg 3, 1031 CM Amsterdam, The Netherlands.

Cu(110)–Ni and Cu(100)–Ni [11,12]. The initial adsorption of O_2 on the latter two surfaces proceeds as on the corresponding Cu surface [12,13]. The reactivity of sorbed oxygen with H_2 on Cu(110)–Ni is enhanced by the presence of Ni with respect to pure Cu(110).

In this paper we report results on the adsorption of O_2 on Cu(111)–Ni and the reactivity of sorbed oxygen with H_2. The interaction of CO with clean and oxygen covered Cu(111)–Ni surfaces will be discussed elsewhere [14].

2. Experimental

The experiments were performed in a standard UHV system with facilities for ellipsometry, Auger electron spectroscopy (AES) and low energy electron diffraction (LEED) [15]. The crystal was disc-shaped, spark-cut within 2° of the (111) orientation from a 5N copper rod, ground and electro-lap polished before mounting in the crystal holder. The surface was cleaned by cycles of sputtering (500 eV, 5 μA/cm^2, 8×10^{-3} Pa Ar, angle of incidence 45°) and annealing (450°C).

Auger spectra were recorded with a four-grid retarding field analyser [11]. The ellipsometric procedure consisted of a continuous measurement of Δ and ψ in one zone with an automatic nulling ellipsometer in the PCSA configuration [13,16]. The wavelength was 632.8 nm and the angle of incidence 70 ± 1°.

Cu(111)–Ni alloys were prepared by admitting a mixture of Ni(CO)$_4$ and CO to the vacuum chamber at a crystal temperature of 220°C. The amount of Ni deposited was continuously monitored with ellipsometry [12]. The surface layers of the alloys were characterised with AES. The results presented in this paper were obtained with Cu(111) surfaces onto which Ni was deposited up to $\delta\psi = 0.4°$. The amount of Ni in the surface was $x_L = 0 \pm 0.05$ and $x_H = 0.20 \pm 0.05$, where x_L is the amount based on the low energy Auger transitions (Ni 101 eV, Cu 105 eV) and x_H is based on the high energy peaks (Ni 720 eV, Cu + Ni 850 eV, Cu 920 eV) using the relative elemental sensitivity factors as given in ref. [17]. These surfaces alloys are denoted as Cu(111)–Ni(0.4)°.

During all gas exposure the gas was continuously renewed by pumping with the turbo-molecular pump.

3. Sorption of O_2 on Cu(111)–Ni(0.4°) surfaces

3.1. Results

Sorption of O_2 on a Cu(111)–Ni(0.4°) surface was studied in the pressure range 10^{-6}–10^{-3} Pa at crystal temperatures varying from 22 to 363°C. Fig. 1 shows an example of the response of the two techniques, ellipsometry and

AES, used to monitor the adsorption of O_2 at a crystal temperature of $65\,^\circ$C and $p = 5 \times 10^{-5}$ Pa. $\delta\Delta$ and $\delta\psi$ are defined as $\overline{\Delta} - \Delta$ and $\overline{\psi} - \psi$, respectively, where $\overline{\Delta}$ and $\overline{\psi}$ are the values for the clean Cu(111)–Ni($0.4\,^\circ$) surface. The AES signal given in fig. 1 corresponds to the ratio of the heights of the oxygen 510 eV signal (h_O) and the Cu 920 eV peak. The Cu 920 eV peak is normalised to 100% Cu in the surface layers to take into account a possible segregation of Ni, which affects the height of the measured 920 eV peak. This corrected peak height is denoted as h_S. That a Ni segregation actually occurs will be shown in section 4. The initial rate of adsorption is more or less independent of the coverage up to $\delta\Delta = 0.6\,^\circ$ after which a rapid decrease in rate is observed. However, no saturation is observed at $\delta\Delta = 0.7\,^\circ$, which is the saturation value for oxygen adsorption on pure Cu(111) [4,8].

The initial stage of chemisorption, up to $\delta\Delta = 0.2\,^\circ$, is strongly affected by the pre-treatment of the crystal. On a freshly prepared Cu(111)–Ni($0.4\,^\circ$) surface the rate of change of Δ is constant up to crystal temperatures of about $100\,^\circ$C. From 100 to $250\,^\circ$C one observes a more or less S-shaped $\delta\Delta$ versus exposure curve, whereas above $250\,^\circ$C the rate of change of Δ steadily increases up to $\delta\Delta = 0.2\,^\circ$, this increase being more pronounced at higher crystal temperatures. This is depicted in fig. 2a. The adsorption of oxygen on a Cu(111)–Ni($0.4\,^\circ$) surface, which has been precovered by oxygen, the oxygen being removed by either H_2 or CO, is characterised by a constant rate of change of Δ for every crystal temperature studied, as can be seen from fig. 2b.

Comparing the initial chemisorption on a freshly prepared surface, the first adsorption and chemisorption on a previously oxidised and reduced surface, the second adsorption, one also observes a difference in the relation between h_O/h_S and $\delta\Delta$ and the relation between x_H and $\delta\Delta$. This is depicted in figs. 2c
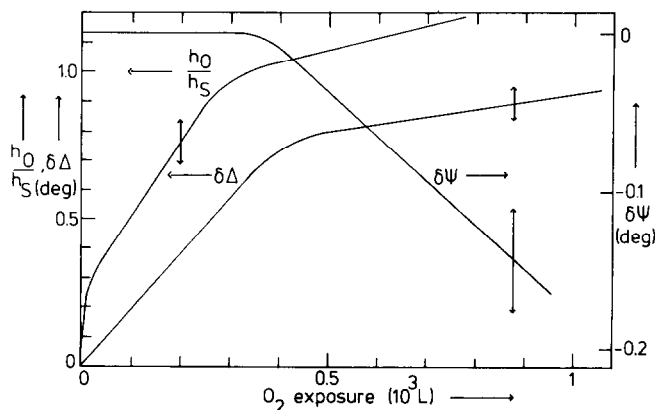

Fig. 1. Oxygen Auger signal h_O/h_S (h_S is the normalised Cu 920 eV peak height), $\delta\Delta$ and $\delta\psi$ versus oxygen exposure at a crystal temperature of $65\,^\circ$C.

and 2d, respectively. From fig. 2c it can be seen that the same change in Δ is accompanied by a far smaller change in h_O/h_S in the second adsorption. Fig. 2d shows an initial decrease in x_H in the first adsorption which is not observed during the second adsorption. These results show that an irreversible change in the surface structure takes place during the first oxygen chemisorption.

In all cases the oxygen coverage was determined by measuring $\delta\Delta$ and h_O/h_S after oxygen exposures and pumping away the gas phase to ensure that the electron gun did not influence the adsorption process. No influence of the operating ionisation gauge on the oxygen uptake curves was observed. Fig. 3 shows the relation between h_O/h_S and $\delta\Delta$ for different crystal temperatures. Also indicated are points obtained after oxygen adsorption directly up to a change in Δ of $1°$ at different crystal temperatures. It can be seen that there is a linear relationship between h_O/h_S and $\delta\Delta$, after the initial adsorption, which, however, is crystal temperature dependent. This means that either $\delta\Delta$ or h_O/h_S or both parameters depend on the crystal temperature.

To determine this dependence the following experiments were carried out. First oxygen was adsorbed at room temperature up to $h_O/h_S = 1.4$ and $\delta\Delta = 1°$. Subsequently h_O/h_S was measured whilst increasing the crystal temperature at background pressure. Fig. 4 shows h_O/h_S and the crystal temperature as a function of time. The temperature increases more or less linearly whereas the AES signal decreases and the rate of decrease increases with increasing temperature. However, it can be seen that almost immediately
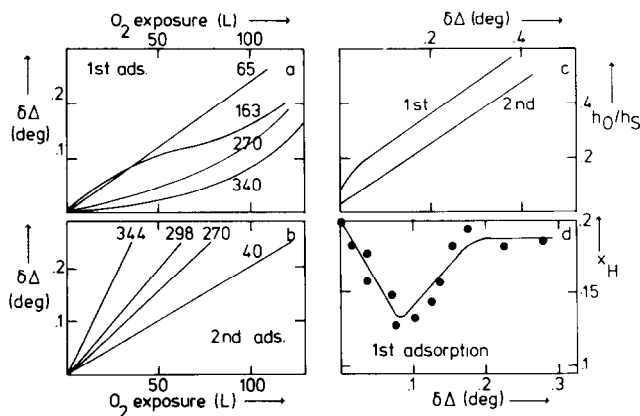

Fig. 2. Initial stage of chemisorption during the first oxygen uptake on a freshly prepared Cu(111)–Ni(0.4°) surface and on a surface which has previously been oxidised and reduced by H_2: (a) $\delta\Delta$ versus exposure at different crystal temperatures during the first adsorption; (b) $\delta\Delta$ versus exposure during the second and following O_2 adsorptions; (c) h_O/h_S versus $\delta\Delta$ during the first adsorption; (d) change in the amount of Ni in the surface layers during the first stage of chemisorption on a freshly prepared Cu(111)–Ni(0.4°) surface.

after the temperature reaches its maximum value and remains constant, the AES signal becomes constant. Also, when the crystal was heated up to an intermediate temperature, the resulting h_O/h_S value corresponded to the intermediate value of fig. 4. Decreasing the crystal temperature causes no change in h_O/h_S. From this experiment we conclude that the measured oxygen Auger signal is a function of the crystal temperature and because of its decrease with increasing temperature it must be due to an irreversible incorporation of oxygen beneath the surface layers of the crystal.
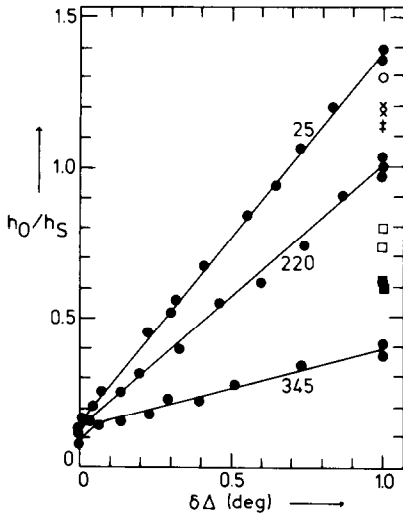

Fig. 3. Relation between the oxygen surface coverage, h_O/h_S, and $\delta\Delta$ for different crystal temperatures.
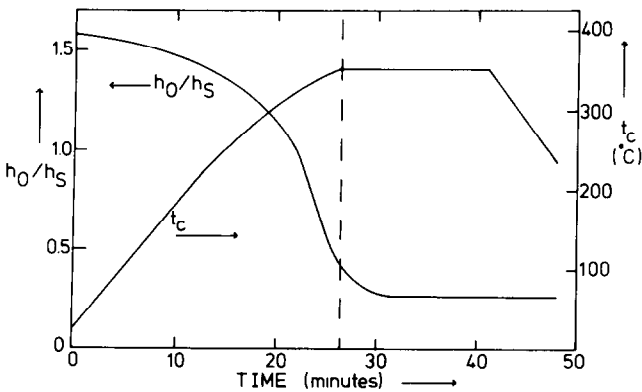

Fig. 4. Change in oxygen surface coverage, h_O/h_S, and the crystal temperature upon heating the crystal with an oxygen content corresponding to $\delta\Delta = 1°$.

It is not possible to investigate the temperature dependence of the ellipso-metric parameter Δ in the same kind of experiment, due to mechanical instabilities of the manipulator. To measure a possible temperature dependence of Δ, oxygen was adsorbed at room temperature up to $\delta\Delta = 1°$. Subsequently the crystal temperature was raised to 240°C and the sorbed oxygen was removed by H_2. Since hydrogen itself does not cause a measurable change in Δ upon adsorption, the observed change in $\delta\Delta$ during exposure of an oxygen covered surface to H_2 is due to the removal of oxygen from the surface. The absolute values of $\delta\Delta$ due to adsorption, were within experimental accuracy, the same as those measured during reaction of sorbed oxygen with hydrogen at a different crystal temperature. From this, one must conclude that the observed change in $\delta\Delta$ depends only on the amount of oxygen and that the $\delta\Delta$ per oxygen atom is not a function of the crystal temperature. The amount of oxygen sorbed is not located at the outermost surface layer but is divided over a (large) number of layers. The coverage of the near surface layers, as determined by AES, decreases with increasing crystal temperature. Since $\delta\Delta$ corresponds to the total amount of oxygen sorbed in the surface and sub-surface layers, this parameter was used to investigate the kinetics of the oxygen adsorption. Fig. 5 shows examples of the oxygen uptake as function of the exposure at different crystal temperatures. The curves include both first and second adsorption experiments. It appears that in the whole temperature region the rate of adsorption, $d(\delta\Delta)/dt$, is proportional to the oxygen pres-sure. Phenomenologically the curves of fig. 5 can be divided into two regions. The first stage up to about $\delta\Delta = 0.5°$, is characterised by a continuous rate of oxygen uptake. The change in ψ is approximately zero and a continuous increase in background intensity of the (1×1) LEED pattern is observed. The
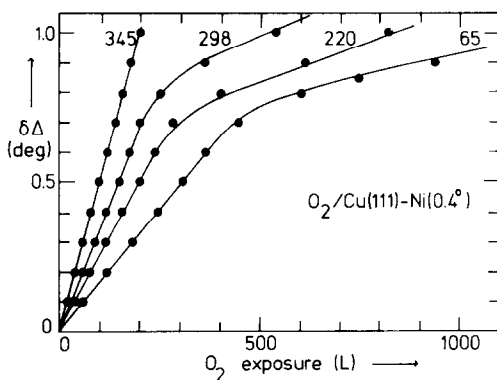

Fig. 5. $\delta\Delta$ versus O_2 exposure at different crstal temperatures. Dots denote the solution of simultaneous integration of eq. (7) and eq. (8).

second stage, above $\delta\Delta = 0.7°$, shows a smaller reaction rate which is, however, much more temperature dependent, while $\delta\psi$ becomes negative.

Apart from the first chemisorption stage, up to $\delta\Delta = 0.2°$, no difference is observed between the first and following oxygen adsorption curves After evacuating the system after an O_2 exposure there is no change in Δ as a function of time. The oxygen Auger signal, however, recorded immediately after evacuation, shows a tendency to decrease as a function of time which is more pronounced at higher crystal temperatures. This implies that relaxation of the adsorbed layer does not take place only during the adsorption process.

3.2. Discussion

The initial chemisorption of oxygen on a freshly prepared Cu(111)–Ni(0.4°) surface causes a reconstruction of the surface layers, as can be deduced from fig. 2. The reconstruction is irreversible; after removing the oxygen from the surface with hydrogen, the second and following oxygen chemisorptions are all characterised by the same constant rate of adsorption. This has also been observed for the pure Cu(111) surface [4]. From theoretical calculations [18] and practical observations [19] it is known that oxygen causes a Ni segregation in Cu–Ni alloys, however, this will only be possible if the Ni atoms which reside in the subsurface layers are in the vicinity of the outermost layer. As pointed out before, the Ni profile in Cu single crystals, prepared by dissociation of Ni(CO)$_4$, can qualitatively be described by [20]:

$$x_{Ni}(i) = Ai \exp(-Bi), \tag{1}$$

where i is the number of the layer, $i = 0$ is the surface layer, and $x_{Ni}(i)$ is the mole fraction of Ni in layer i. A and B are constants depending on the total amount of Ni deposited and the crystal temperature. This profile is more contracted for Cu(111) than Cu(110) [11] for the same amount of Ni deposited. This means that on the average Ni in the subsurface layers of Cu(111) is nearer to the surface than Ni in Cu(110). The segregation of Ni caused by CO, which takes place at much lower pressures on Cu(111)–Ni(0.4°) [14] than on Cu(110)–Ni(1°) [21] supports this explanation of the initial surface reconstruction in Cu(111)–Ni(0.4°) which was not observed during oxygen adsorption on Cu(110)–Ni(1°).

Since a redistribution of Ni causes a negative change in $\delta\Delta$ [11], the first initial adsorption of oxygen may be described by the following processes:
(1) At low temperature where Ni segregation is kinetically limited and virtually absent, adsorption takes place as on pure Cu(111) (cf. fig. 2a for 65°C).
(2) At high crystal temperatures we find an apparently increasing adsorption rate because of an immediate rearrangement of the metal atoms in the surface layers which counteracts the positive change in $\delta\Delta$ due to oxygen adsorption (cf. fig. 2a above 270°C).

(3) An intermediate case at crystal temperatures between these two extremes.

The absolute oxygen coverage cannot be experimentally determined because of the absence of an ordered LEED pattern at a known coverage. From the proportionality between $\delta\Delta$ and h_O/h_S, the temperature independence of $\delta\Delta$ and the relation between θ_O and $\delta\Delta$ for oxygen adsorbed on pure Cu(111) [4] we assume the following relation between the oxygen content and $\delta\Delta$:

$$\theta_O = 0.7\,\delta\Delta, \tag{2}$$

where θ_O is the total oxygen concentration, i.e. the sum of the amount of oxygen chemisorbed at the surface θ_c (= the number of oxygen atoms at the surface per surface atom) and the amount of incorporated oxygen θ_i (= the number of oxygen atoms per surface atom in subsurface layers).

Chemisorption of oxygen on Cu(111) could be described by an equation derived by Kohrt and Gomer [22] for dissociative adsorption via a mobile precursor state, requiring a pair of adjacent free sites [4]:

$$s(\theta') = s(0)\,(1 - \theta')^2 / \left[(1 - \theta')^2 + K'\theta' + K''\theta'(1 - \theta')\right], \tag{3}$$

where $s(\theta')$ is the sticking probability at coverage θ', $s(0)$ is the sticking probability at zero coverage and θ' is related to the maximum coverage by

$$\theta' = \theta_c/\theta_{c,m}, \tag{4}$$

where $\theta_{c,m} = 0.5$. K' and K'' are constants related to the probabilities of desorption from a filled site (K') and an empty site not available for adsorption (K''):

$$K' = P_d'/(P_a + P_d), \quad K'' = P_d''/(P_a + P_d), \tag{5}$$

where P_a and P_d are respectively the probabilities for adsorption and desorption from the precursor state at a site available for adsorption, P_d' and P_d'' are respectively the probabilities for desorption from a filled site and an empty site not available for adsorption (i.e. a site whose next neighbour site is filled).

The oxygen chemisorption on Cu(111) [4], Cu(110) and Cu(110)–Ni(1°) [13] have been described with this model with $K' = K'' = 0.02$, the only difference being the initial sticking probability. Although no saturation of oxygen chemisorption occurs on Cu(111)–Ni(0.4°), the initial oxygen uptake curves shown in fig. 5 could be fitted with the model described above. The incorporation of oxygen can be described by the addition of a simple first order reaction:

$$O_c \underset{k_2}{\overset{k_1}{\rightleftarrows}} O_i. \tag{6}$$

This leads to the following kinetic expressions for oxygen sorption on Cu(111)–Ni(0.4°):

$$d\theta_c/dt = (\phi/N_s)\,s(0)\,(1 - \theta')^2 / \left[(1 - \theta')^2 + K\theta'(2 - \theta')\right] - k_1\theta_c + k_2\theta_i, \tag{7}$$

$$d\theta_i/dt = k_1\theta_c - k_2\theta_i. \tag{8}$$

The results of simultaneous integration of eqs. (7) and (8) are shown in fig. 5 with $K = 0.02$ and $s(0)$ as determined from the initial slope of $\delta\Delta$ versus exposure curves. ϕ is the flux of oxygen atoms and N_s is the nubmer of surface atoms. From the value or the parameters k_1 and k_2, obtained from the fit procedure, one should be able to determine the ratio θ_c/θ_i at any time and temperature during oxygen adsorption. However, the model is not very sensitive to the precise value of k_2, for k_2 smaller than k_1. Within experimental accuracy, fits could be obtained even for k_2 equal to zero. This value, however, is physically not allowed because incorporated oxygen can also be removed from the surface. The amount of oxygen at the surface versus the crystal temperature, which can be derived from fig. 4, indicates that apparent activation energy of k_2 has to be smaller than that of k_1 because θ_c/θ_i decreases with increasing temperature at a constant amount of oxygen sorbed. Since it is not possible to evaluate an unequivocal temperature dependence of k_2 from the fit procedure one cannot compare the results with those obtained from fig. 4.

The value of $K = 0.02$ is equal to the value used to fit the oxygen adsorption on Cu(111) and Cu(110)–Ni(1°), indicating that the probabilities of desorption from filled sites and from sites not available for adsorption are very small for both Cu(111)–Ni and Cu(110)–Ni. If one assumes that the condensation coefficient is independent of the crystal temperature, as is observed for $N_2/W(100)$ [23], the probability of desorption has to have an appreciable value compared to the probability of adsorption because of the temperature dependence of $s(0)$:

$$s(0) = \alpha P_a/(P_a + P_d),\tag{9}$$

where α is the condensation coefficient. The temperature dependence of $s(0)$ is depicted in an Arrhenius plot in fig. 6. The apparent activation energy increases with increasing crystal temperature as was also observed for O_2 adsorption on pure Cu(111) [4] which is also indicated in fig. 6. The change in apparent activation energy could be due to a difference in activation energies of the probabilities for adsorption and desorption, the latter being smaller, or due to a change in the condensation coefficient.

The large rate of incorporation of oxygen on Cu(111)–Ni(0.4°) with respect to pure Cu(111), where sorption beyond half a monolayer is only observed for oxygen pressures above 10^{-2} Pa, has to be ascribed to the presence of Ni in subsurface layers which facilitates the incorporation of oxygen. This was also observed for oxygen adsorption on Cu(100)–Ni(0.7°) and Cu(110)–Ni(1°) with respect to the pure Cu surfaces [12,13]. It is questionable whether the depth profile of the incorporated oxygen could be established from sputter experiments, since the system contains in fact three components (oxygen, copper and nickel). This will yield difficulties in defining an unambiguous sputter coefficient.

The interaction of a gas like O_2, CO or H_2, with the surface of a Cu–Ni

alloy is able to change the composition of the alloy surface. This has already been observed for CO adsorption on Cu–Ni films [24] and was also observed for Cu–Ni single crystal alloys prepared by $Ni(CO)_4$ decomposition [14,21]. In case of oxygen adsorption on Cu(110)–Ni, where the kinetics of the second oxygen uptake differ from the first one, we pointed out that this was due to a change at the surface which had taken place after removal of the first amount of oxygen sorbed. For Cu(111)–Ni it follows from fig. 2 that the change in surface composition actually takes place during the first oxygen adsorption.

4. Segregation of Ni induced by O_2 adsorption

4.1. Results

The change in surface composition of Cu(111)–Ni(0.4°) surface alloys, induced by oxygen adsorption, was investigated with AES. Table 1 shows the values of x_H and $h'_{106} = h_{106}/h^0_{106}$ is the peak-to-peak height of the Cu 106 eV peak after preparation of the Cu(111)–Ni(0.4°) alloy surface, for different temperatures, before and after oxygen adsorption and removal of oxygen from the surface by H_2 or CO. The height of the Ni 101 eV peak, which is practically zero for the clean Cu–Ni surface because of the small amount of Ni deposited, was more or less constant or slightly increased after oxygen adsorption. It can be seen that the decrease in the 106 eV peak becomes smaller within increasing crystal temperatures, after oxygen adsorption. The decrease in the amount of Ni in 6 8 layers, x_H, increases with increasing adsorption temperatures. After reduction of the surface, the height of the 106 eV peak is
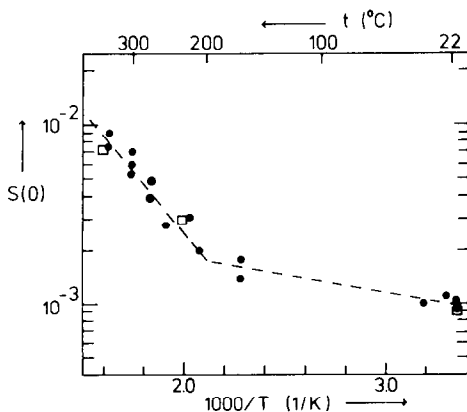

Fig. 6. Arrhenius plot of the initial sticking probability of O_2 on: (●) Cu(111)–Ni(0.4°); (□) pure Cu(111).

Table 1
Variation in surface composition due to oxygen adsorption

t_C (°C)	"Clean"		First adsorption		First reduction		Second adsorption		Second reduction	
	x_H	h'_{106}	x_H	h'_{106}	x_H	h'_{106}	x_H	h'_{106}	x_H	h'_{106}
160	0.22	1	0.18	0.5	0.21	1.0	0.19	0.5	0.22	0.9
220	0.22	1	0.17	0.5	0.22	1.0	0.18	0.5	0.21	1.1
260	0.20	1	0.16	0.7	0.19	1.3	0.15	0.6	0.19	1.0
300	0.21	1	0.06	0.8	0.12	1.1	0.03	0.7	0.13	1.0
340	0.18	1	0.05	0.9	0.07	1.0	0.03	0.9	0.06	0.9

increased to about the height before oxygen adsorption. When the surface was reduced with CO we did not observe a significant increase in the Ni 101 eV peak due to Ni segregation, because of the relatively low CO pressures used. The value of x_H also increases after reduction. However, after reduction at more elevated temperatures, this increase is smaller and does not equal the decrease observed after the first oxygen adsorption.

4.2. Discussion

The decrease in the Cu 106 eV signal after oxygen adsorption can be explained by an attenuation of the copper signal by oxygen atoms: in the first few surface layers copper atoms are screened by oxygen atoms. However, then one would expect an equal attenuation of the Ni 101 eV peak, which is not observed since whenever a significant change in the 101 eV signal occurs, it is an increase rather than a decrease after oxygen adsorption. It is also not possible to explain the lack of attenuation of the Ni 101 eV peak by simply stating that the appearance of the 101 eV signal is due to Ni in deeper layers since we have shown that oxygen penetrates to deeper layers and one would expect the same attenuation of oxygen in those deeper layers. Since it is not possible to explain the decrease in the Cu signal together with the invariance, or increase, of the Ni signal, by a simple attenuation of the metal Auger signals caused by oxygen, we propose that the observations may be explained by a Ni segregation to the surface. The attenuation of the Ni 101 eV signal, caused by oxygen, is compensated by segregation of Ni to the surface, whereas the attenuation of the Cu 106 eV signal is enhanced by an increased Ni content at the surface.

The change in x_H resembles the change in composition which was observed after oxidation and reduction of Cu(100)–Ni(0.7°). That is, a decrease in x_H after oxygen adsorption whose value is more or less restored after reduction. This decrease was explained by a specific attenuation of the Ni signal in deeper layers. However, it is also possible that Ni, facilitating the incorporation of oxygen (section 3, refs. [12,13]), accompanies the penetrating oxygen atoms.

This results in a migration of Ni atoms to still deeper layers and thus in a decrease in x_H.

5. Reaction of hydrogen with oxygen sorbed on Cu(111)–Ni(0.4°)

5.1. Results

Cu(111)–Ni(0.4°) surfaces containing different amounts of oxygen, were exposed to hydrogen in the pressure range from 2×10^{-3} to 4×10^{-1} Pa at crystal temperatures varying between 163 and 350°C. Fig. 7 shows some typical reaction curves measured at different crystal temperatures, starting with an oxygen coverage corresponding to $\delta\Delta = 1°$, as a function of time. The hydrogen pressures have been corrected for the ionisation gauge sensitivity. It can be seen that at relatively low crystal temperatures the initial reaction rate is apparently zero, increasing to a maximum rate at $\delta\Delta \sim 0.5°$, after which the rate steadily decrease to zero. At crystal temperatures above 300°C the initial reaction rate is finite as shown in the insert of fig. 7, increasing with decreasing oxygen coverage to a maximum, after which the rate decreases to zero. Auger spectra recorded after prolonged hydrogen exposures, when no more change in $\delta\Delta$ could be observed, showed only small amounts of oxygen ($\theta_O < 0.03$), comparable to the amount present on the clean surface before oxygen adsorption. From the observation that the increase in $\delta\Delta$, accompanying the adsorption of oxygen, is equal to the decrease in $\delta\Delta$, due to removal of the sorbed oxygen with hydrogen one can conclude that hydrogen removes the oxygen quantitatively.
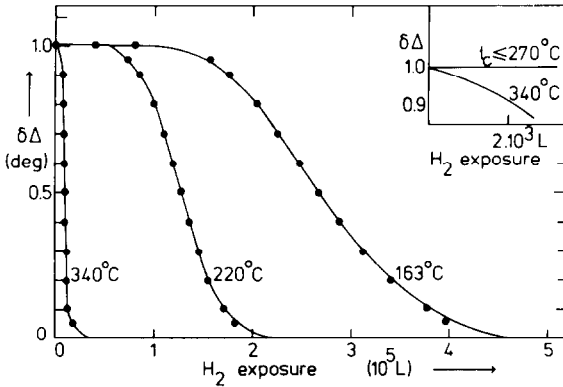

Fig. 7. $\delta\Delta$ versus H_2 exposure to a Cu(111)–Ni(0.4°) surface covered with oxygen up to $\delta\Delta = 1°$, at different crystal temperatures. Dots denote fits of eq. (11) with $n = 3$, $m = 2$. The values of α are indicated in table 2.

When hydrogen was readmitted after evacuation of the system, before the completion of the reaction, the initial rate of reaction corresponded to the rate before evacuation. It was not possible to observe a continuing reaction with adsorbed hydrogen after evacuation because of the low pumping speed for hydrogen.

The extent of the reaction and the reaction rate are strongly influenced by an operating ionisation gauge, although the gauge was not in line of sight with the crystal surface. Fig. 8 shows two reaction curves both recorded at a crystal temperature of 270°C, hydrogen pressure of 10^{-2} Pa and an initial oxygen coverage corresponding to $\delta\Delta = 1°$. The initial rate of reaction increases from apparently zero to a finite value when the gauge is operating. Also the rate at intermediate coverages is considerably larger with an operating ionisation gauge. In the region of an apparent zero reaction rate the reduction of the surface can be "started" and "stopped" simply by switching the gauge on and off.

The dependence of the reaction rate, $d(\delta\Delta)/dt$, on the H_2 pressure was investigated at constant temperature. Fig. 9 shows the maximum rate, at the inflection point, as a function of pressure. The slope of the curve is 0.65 ± 0.1 independent of the reaction temperature.

5.2. Discussion

The most striking feature of the kinetics of the reaction of hydrogen with oxygen sorbed on Cu(111)–Ni(0.4°) is the difference in hydrogen reaction order compared with the same reaction on Cu(110)–Ni(1°). For Cu(110)–Ni(1°) the reaction order with respect to hydrogen was 1 and the
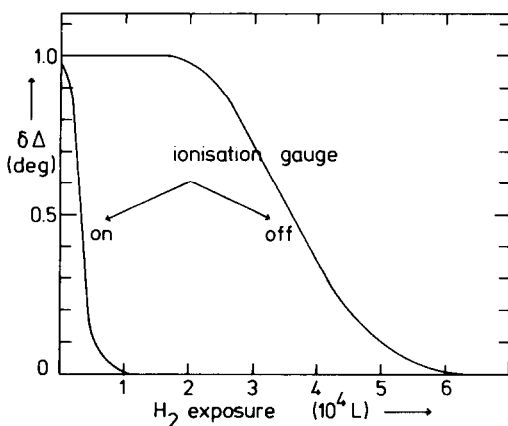

Fig. 8. Influence of an operating ionisation gauge on the reduction of O/Cu(111)–Ni(0.4°) with H_2.

reaction rate independent of the oxygen coverage for θ_O smaller than 0.5. This was explained by hydrogen dissociation being the rate determining step, taking place at a "Ni like" site. Hydrogen atoms then react with oxygen on "Cu like" sites [13], since the activation energy for this step was found to be the same as that on pure Cu(110) [7]. The reaction rate of hydrogen with oxygen on pure Cu(111) was also first order in the hydrogen pressure, hydrogen dissociation being the rate determining step. In this case, however, the rate of hydrogen dissociation also depends on the oxygen coverage of the surface [8]. The removal of oxygen from Cu(111)–Ni(0.4°) with hydrogen does not resemble any of the above mentioned systems. Rather, it is similar to the reduction of O/Ni(111) and O/Ni(100) [5,9]. This may not be surprising, considering the fact that on Cu(111)–Ni(0.4°) a larger amount of Ni is present in the near surface region compared with Cu(110)–Ni(1°) [11], and an oxygen induced Ni segregation occurs on the (111) alloy surface (c.f. section 4).

The model used to describe the reduction of oxidised Ni surfaces is a nucleation and growth type mechanism [25], or a more refined version of this [9]. For the sake of simplicity we will use the original approach, as given by Avrami [25]. The growth of clean Ni islands is governed by the following general expression:

$$\theta_{Ni}(t) = \theta_{Ni}(0)\left[1 - \exp(-\alpha p^m t^n)\right], \tag{10}$$

or, in terms of the oxygen coverage:

$$\theta_O(t) = \theta_O(0) \exp(-\alpha p^m t^n), \tag{11}$$

where α is a constant, depending only on temperature and the details of the reaction, p is the hydrogen pressure and m and n are constants.
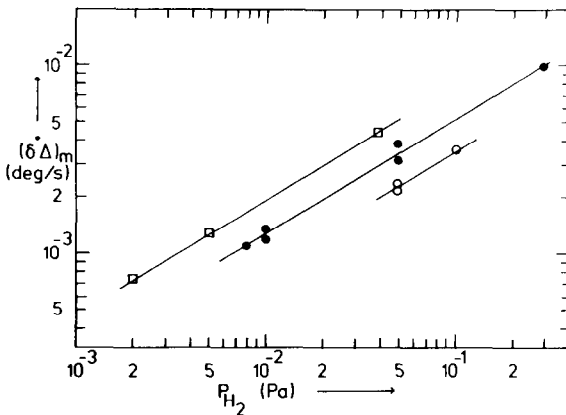

Fig. 9. Reaction rate $d(\delta\Delta)/dt$ versus the H_2 pressure at different crystal temperatures. The slope of the lines is 0.65 ± 0.1.

For two-dimensional growth, starting from a given number of centres, all present at $t = 0$, n should be equal to 2. However, from our observed reaction curves at constant temperature and pressure, a value of $n = 3$ is obtained. This can be explained either by assuming a three-dimensional growth process, or by a continuing creation of active centres, from which two-dimensional growth can start at all times. The former alternative is unlikely in view of the fact that the bulky water molecules formed in the reaction are not easily transported to the surface in order to desorb. The latter hypothesis is not unreasonable, since the oxide formed on the alloy surface will certainly be less well ordered than that on pure Ni(111) or Ni(100), where epitaxial relations and LEED patterns have been reported [5]. The possibility of creating a new growth centre in a disordered layer can certainly not be discarded.

The pressure dependence of the reaction rate, as given by the slope at the inflection point of eq. (11) is easily derived to be proportional to $p^{m/n}$. Using the experimental values of m/n (= 0.65, cf. fig. 9) and $n = 3$, we obtain $m = 2$. As can be seen from fig. 7, these constants can be used to fit the whole of the experimental reaction curves. The temperature dependence of α (in Torr $^{-2}$ s^{-3}), given in table 2, is then found to be:

$$\ln \alpha = (8.5 \pm 2) - (4.7 \pm 1) \times 10^3 / T, \tag{12}$$

which yields an activation energy of 9 ± 2 kcal/mol.

The physical meaning of the activation energy and the value of $m = 2$, can be obtained from the complete expression for $\theta_O(t)$, appropriate to our case:

$$\theta_O(t) = \theta_O(0) \exp\left[-\nu N(0) \pi (\mathrm{d}r/\mathrm{d}t)^2 t^3 \right], \tag{13}$$

where $1/\nu$ is the average time between the creation of active centres, $N(0)$ the number of sites per unit area available for growth at $t = 0$ and $\mathrm{d}r/\mathrm{d}t$ the radial growth rate of the clean nickel islands. It is logical to assume, as before [5,9], that $(\mathrm{d}r/\mathrm{d}t)$ is proportional to the surface hydrogen concentration H_{ad}. Now two cases may be envisaged. If a dissociative hydrogen adsorption equilibrium is established, as on O/Ni(111) and O/Ni(100) [5,9], $H_{ad} = Kp^{1/2}$ and we must conclude that ν is proportional to the hydrogen pressure in order to arrive at the observed p^2 dependence. If, on the other hand, ν is independent of the hydrogen pressure, one should have $\mathrm{d}r/\mathrm{d}t \sim p$. Taking the dissociation equi-

Table 2

Values of α required to fit the experimental curves with eq. (11) and $m = 2$ and $n = 3$

Crystal temperature (°C)	α (Torr^{-2} s^{-3})	Crystal temperature (°C)	α (Torr^{-2} s^{-3})
344	2.1	220	0.29
298	1.1	182	0.16
270	0.72	163	0.082

librium into account, $H_{ad}^2 \sim p \sim dr/dt$, this implies the occurrence of a tri-molecular reaction which is not likely. Assuming hydrogen dissociation to be rate limiting, as on Cu(110)–Ni and pure Cu, will lead to $dr/dt \sim p$. The first explanation of the p^2 dependence, ν being proportional to the hydrogen pressure, seems most likely because we did not observe a significant increase in the number of active centres in the absence of a hydrogen gas phase. If hydrogen dissociation is the rate limiting step and the creation of new active centres is independent of the hydrogen pressure, one expects a large influence of the delay time between the oxygen adsorption and the start of the reduction reaction. Since no significant influence of the delay time is observed, which time was of the order of the time required for the reduction reaction, it is not likely that the active centre generation is independent of the hydrogen pressure. We are then left with the conclusion that the reduction of oxidised Cu(111)–Ni(0.4°) takes place via adsorbed hydrogen atoms, in equilibrium with the gas phase, as on Ni(111) and Ni(100). The difference in reduction behaviour with respect to Cu(111) and Cu(110)–Ni has to be ascribed to the relative large amount of nickel present in the near surface region of the (111) alloy surface.

The nucleation frequency ν for centres, where the reduction process starts, is also proportional to the hydrogen pressure, i.e. proportional to the number of collisions per second with the surface, $\nu = \nu_0 p$. The observed activation energy $E_{exp} = 9 \pm 2$ kcal/mol is that of the factor

$$\nu N(0) \, \pi (dr/dt)^2 p^{-2}.$$

In the case of pure Ni(100) or Ni(111) the corresponding quantity $N(0)\pi(dr/dt)^2 p^{-1}$ has an appreciably higher activation energy (viz. 23 kcal/mol). In our case the observed activation energy contains that of ν, which is unknown, and can therefore not easily be interpreted in terms of more basic quantities. According to the analysis given earlier [5], the actual rate limiting step with rate constant k_r will have an activation energy $E_r = \frac{1}{2}(9 + E_{ad}(H_2) - E_\nu)$ on the alloy surface, compared to $\frac{1}{2}(23 + E_{ad}(H_2))$ for the same reaction on pure Ni. It thus seems that, as the rate limiting step is no longer the dissociation of hydrogen, the presence of copper in the surface facilitates the reduction of the surface. Comparing the numerical values of α for the alloy surface and pure nickel we find:

$$\nu_0 = \left[N(0)k_r^2 \right]_{Ni} / \left[N(0)k_r^2 \right]_{alloy} \times 0.1 \text{ Torr}^{-1} \text{ s}^{-1}. \tag{14}$$

For a typical reaction time of 10^3 s at a pressure of 10^{-4} Torr we have $\nu t = \nu_0 pt \ll 10^{-2}$, since both the density of nuclei $N(0)$ and the rate constant k_r will be larger on the alloy surface. This condition is actually necessary for eq. (13) to be valid. It thus follows that our description is indeed self-consistent.

Acknowledgements

References

[1] G. Ertl and J. Küppers, Surface Sci. 24 (1971) 104.
[2] C.R. Helms and K.Y. Yu, J. Vacuum Sci. Technol. 12 (1975) 279.
[3] Y. Takasu, H. Shimizu, S. Mazu and Y. Matsuda, Surface Sci. 61 (1976) 279.
[4] F.H.P.M. Habraken, E.Ph. Kieffer and G.A. Bootsma, Surface Sci. 83 (1979) 45.
[5] P.K. de Bokx, F. Labohm, O.L.J. Gijzeman, G.A. Bootsma and J.W. Geus, Appl. Surface Sci. 5 (1980) 321.
[6] F.H.P.M. Habraken and G.A. Bootsma, Surface Sci. 87 (1979) 333;
    F.H.P.M. Habraken, C.M.A.M. Mesters and G.A. Bootsma, Surfce Sci. 97 (1980) 264.
[7] S. Hachicha, P. Hofmann and A.M. Bradshaw, in: Proc. IVC-8, ICSS-4, ECOSS-3, Cannes, 1980, p. 489.
[8] C.M.A.M. Mesters, T.J. Vink, O.L.J. Gijzeman and J.W. Geus, Surface Sci. 135 (1983) 428.
[9] F. Labohm, O.L.J. Gijzeman and J.W. Geus, Surface Sci. 135 (1983) 409.
[10] F. Labohm, C.W.R. Engelen, O.L.J. Gijzeman, J.W. Geus and G.A. Bootsma, J. Chem. Soc. Faraday Trans. I, 78 (1982) 2435.
[11] C.M.A.M. Mesters, G. Wermer, O.L.J. Gijzeman and J.W. Geus, Surface Sci. 135 (1983) 396.
[12] C.A. Pietersen, C.M.A.M. Mesters, F.H.P.M. Habraken, O.L.J. Gijzeman, J.W. Geus and G.A. Bootsma, Surface Sci. 108 (1981) 197.
[13] C.M.A.M. Mesters, A.F.H. Wielers, O.L.J. Gijzeman, G.A. Bootsma and J.W. Geus, Surface Sci. 117 (1982) 605.
[14] C.M.A.M. Mesters, A. de Koster, O.L.J. Gijzeman and J.W. Geus, Appl. Surface Sci. 20 (1984) 1.
[15] F.C. Schouten, E.W. Kaleveld and G.A. Bootsma, Surface Sci. 63 (1977) 460.
[16] H. Albers, J.M.M. Droog and G.A. Bootsma, Surface Sci. 64 (1977) 1.
[17] P.R. Webber, L.E. Rojas, P.F. Dobson and D. Chadwick, Surface Sci. 105 (1980) 20, and references therein.
[18] D. Tománek, S. Mukherjee, V. Kumar and K.H. Bennemann, Surface Sci. 114 (1982) 11.
[19] G. Ertl, in: The Nature of the Surface Chemical Bond, Eds. T. Rhodin and G. Ertl (North-Holland, Amsterdam, 1980).
[20] O.L.J. Gijzeman and H.N.W. Lekkerkerker, Chem. Phys. Letters 95 (1983) 52.
[21] C.M.A.M. Mesters, A.F.H. Wielers, O.L.J. Gijzeman, J.W. Geus and G.A. Bootsma, Surface Sci. 115 (1982) 237.
[22] C. Kohrt and R. Gomer, J. Chem. Phys. 52 (1970) 3283.
[23] D.A. King and M.G. Wells, Proc. Roy. Soc. (London) A339 (1974) 245.
[24] F.J. Kuijers and V. Ponec, Surface Sci. 68 (1977) 294.
[25] M. Avrami, J. Chem. Phys. 7 (1939) 1103; 8 (1940) 212; 9 (1941) 177.